Melting phenomenon in laser-induced shock waves

Zohar Henis and Shalom Eliezer
Plasma Physics Group, Soreq Nuclear Research Center, Yavne 70600, Israel
(Received 21 April 1993)

The melting fraction in laser-induced shock waves in aluminum was estimated as a function of the shock pressure. The results show that partial melting can begin during the relaxation of a shock pressure of 680 kbar. It is also suggested that for very short laser pulses (femtoseconds) a supercooling phenomenon may occur without melting during the rarefaction wave.

PACS number(s): 52.50.Jm, 64.70.Dv

The study of matter under extreme conditions is an interdisciplinary subject with important applications [1,2] to material science, astrophysics, geophysics, nuclear physics, plasma physics, and in applied sciences such as fission, fusion, etc. The physics of high pressure is studied experimentally in the laboratory using static and dynamic techniques. In static experiments [3] the maximum presently obtained pressures are about 2 Mbar and the temperatures are up to a few hundred degrees Celsius. In the dynamic experiments shock waves are created [4–6]. Chemical explosives have been used to create shock waves up to about 10 Mbar in metals with accompanying temperatures of the order of 10^4 K, while high-power layers [7,8] have achieved up to 100 Mbar pressures. An interesting feature of the laser-driven shock waves is the short and tunable laser-pulse duration implying the possibility of studying high-pressure time-dependent phenomena.

In the present work the phenomenon of melting in a laser-induced shock wave is analyzed. The maximum laser-generated shock-wave pressures P_s obtained in an aluminum target can be approximated by the equation [9]

$$P_s(\text{Mbar}) = \frac{12.25[I_L/(10^{14}\ \text{W/cm}^2)]^{0.785}}{1+0.0057[I_L/(10^{14}\ \text{W/cm}^2)]^{-0.725}}\ , \qquad (1)$$

where I_L is the absorbed laser irradiance. For example for $I_L = 10^{13}$ W/cm^2 one obtains 1.95 Mbar, while for $I_L = 10^{12}$ W/cm^2, $P_s = 0.28$ Mbar. In this regime of pressures the Hugoniot curve of aluminum passes into the region of the liquid phase [4,10]. Laser irradiances in the domain of 10^{12}–10^{13} W/cm^2 are easily achieved [7,11]. So far the laser-induced shock-wave experiments were done with nanosecond laser-pulse duration (0.5 to a few ns). Assuming a thermodynamic length scale l_m for melting [12] of the order of 10 μm and a second of sound c of 10^6 cm/s (appropriate for the 1-Mbar regime) one obtains a time scale t_m for melting

$$t_m \sim l_m/c \sim 1\ \text{ns} \qquad (2)$$

of the same order of magnitude as the laser-pulse duration in the present experiments. In this domain of parameters melting is expected and the melting fraction of shocked aluminum is calculated as a function of the Hugoniot pressure.

The phase diagram of aluminum is illustrated in Fig. 1. The Hugoniot (H) and the calculated melting curve (MC) are taken from Ref. [4]. Four shock and the following release paths (rarefaction waves) are also shown in the figure to illustrate the possible different responses of the shocked metal. The primed states represent the final temperatures attained after release. Material following shock 1 remains solid both during shock compression and relaxation from this state since the final temperature 1′ is less than the melting temperature at normal pressure. Metal following shock 2 can evolve in the two following ways: (a) The system releases on the solid isentrope to the intersection (point i) with the melting curve and then it starting melting. As the melting starts the system evolves on the melting curve to the final state 2′. At this point the system can be a mixture of solid and liquid

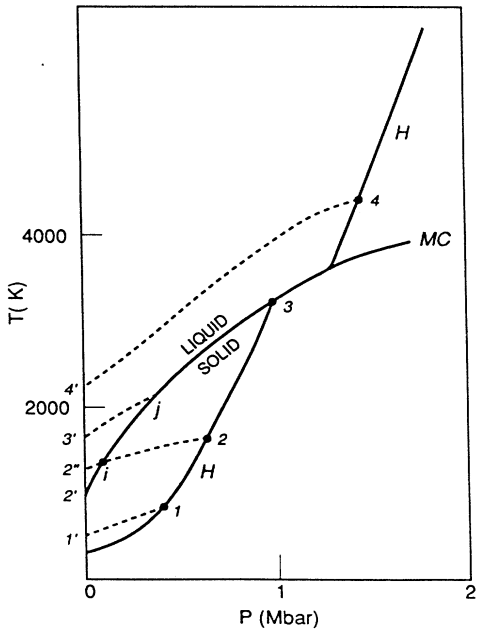

FIG. 1. The aluminum melting curve (MC) and the Hugoniot curve (H) in a temperature (T)–pressure (P) diagram. 11′ and $2i2''$ are rarefaction waves in solid following shock waves from 1 and 2 accordingly. 44′ and $j3'$ are rarefaction waves in liquid.

phases. (b) The system releases on the solid isentrope, passes through the intersection (point i) with the melting curve, and continues to expand along the same adiabat as a supercooled solid to the final temperature 2''. In this case melting does not occur. A similar phenomenon was described by Altshuler *et al.* [13] regarding evaporation of shock-compressed lead during a release wave. Complete melting occurs in the system following the shock (point 3) during its evolution on the melting curve down to point j. Then the system expands on the liquid adiabat to the final temperature 3'. In the shock (point 4) the metal goes into the liquid phase under shock compression and then expands on a liquid adiabat to the final temperature 4'.

Here the possibility of partial melting during relaxation (as illustrated by shock 2 of Fig. 1) is considered. The fraction of metal that melts during the evolution between the points i and 2' is estimated by

$$\lambda=\int_i^{2'}\frac{c_V dT+pdV}{L}\ , \tag{3}$$

where c_V is the specific heat of the metal, T is the temperature, p is the pressure, pdV is the work done due to expansion of the solid and L is the latent heat at the temperature T on the melting curve. The integral of Eq. (3) is calculated along the MC. The latent heat L is given by the Clausius-Clapeyron equation:

$$\frac{dP}{dT}=\frac{L}{T(V_l-V_s)}\ , \tag{4}$$

where V_l and V_s are the specific volumes of the liquid and the solid phases. The latent heat L was calculated as a function of P (or T) on the melting curve using Eq. (4), where dP/dT is taken from the MC of Fig. 1. V_l and V_s were determined on the MC by the liquid [10] and solid [14] equations of state (EOS).

The pressure of the solid is given by [1]

$$P=P_c(V_s)+\frac{\gamma(V_s)}{V_s}[c_V(T-T_0)+E_0]+\frac{1}{4}\left[\frac{\beta_0}{V_0}\right]\left[\frac{V_0}{V_s}\right]^{1/2}T^2\ . \tag{5}$$

$P_c(V_s)$ is the cold pressure of the solid:

$$P_c=\sum_i a_i\delta^{i/3+1}\ , \tag{6}$$

where the coefficients a_i are found from the properties of the material at normal conditions. δ is given by

$$\delta=\rho/\rho_{\rm cr}\ , \tag{7}$$

where $\rho_{\rm cr}$ is the solid density at $T=0$ and $P=0$ and $\rho=1/V_s$ is the solid density. $1/V_0$ is the normal density at room temperature T_0. The numerical values of the solid EOS parameters from Eqs. (5)–(7) for aluminum are listed in Table I. $\gamma(V_s)$ is the Gruneisen coefficient calculated from

$$\gamma(V_s)=-\frac{2}{3}-\frac{V_s}{2}\frac{dP_c^2}{dV_s^2}\Big/\frac{dP_c}{dV_s}\ . \tag{8}$$

TABLE I. Numerical values of the solid EOS of aluminium.

c_V (10^6 erg g^{-1} deg^{-1})	8.96
E_0 (10^7 erg g^{-1})	161.0
β_0 (erg g^{-1} deg^{-2})	500
$\rho_{\rm cr}$ (g cm^{-3})	2.744
$1/V_0$ (g^{-1} cm^3)	1/2.711
T_0	300 K
a_1 (Mbar)	−8.725
a_2 (Mbar)	39.127
a_3 (Mbar)	−69.241
a_4 (Mbar)	56.589
a_5 (Mbar)	−20.346
a_6 (Mbar)	2.696

V_s was solved from Eq. (5) for P and T given on the melting curve (Fig. 1).

The liquid EOS was taken from Ref. [10]:

$$3RT\ln\alpha=P(V_l-V_s)\ , \tag{9}$$

$$\alpha=(1+z)^{-1/2}\exp[b-f(\delta)T_m/T]\ , \tag{10}$$

$$z=lRT\left[\frac{dP_c}{d\rho}-\frac{2}{3}n\frac{P_c}{\rho}\right]^{-1}\ , \tag{11}$$

$$f(\delta)=c+\frac{a}{r}\left[\left[\frac{\delta}{\delta_l}\right]^r-1\right]\ . \tag{12}$$

$\delta_l=V_{l0}/V_1$, where V_{l0} is the liquid specific volume at atmospheric pressure and at the melting temperature. a, b, c, l, n, and r are empirical constants given in Table II for aluminum.

V_s from the solution of Eq. (5) is inserted in Eq. (9) and the V_l values on the melting curve are calculated. These values of V_l and V_s are substituted in Eq. (4) and the calculated latent heat L is plotted in Fig. 2. One can see from Fig. 2 that L is an increasing function of P (or T) and its values change by at most a factor of about 5 along the melting curve.

The melting fraction λ defined in Eq. (3) was calculated as a function of the pressure on the Hugoniot curve. After the shock compression (e.g., point 2) a rarefaction wave follows described by the solid isentrope:

$$T(\rho)=T_H\exp\int_{\rho_H}^{\rho}\gamma(\rho)/\rho\,d\rho\ , \tag{13}$$

where T_H and ρ_H are the temperature and the density on the Hugoniot curve. From Eq. (5) on the MC and Eq. (13) the intersection of the MC and the isentrope were calculated. Two such isentropes are shown in Fig. 1 (lines 1-1' and 2-2'').

The calculated melting fraction as a function of the Hugoniot pressure is shown in Fig. 3. One can see that partial melting during relaxation begins at a shock pressure of about 680 kbar. Total melting upon release

TABLE II. Numerical values of liquid EOS parameters for aluminum.

a	b	c	n	l	r	V_{l0} (cm^3/g)
1.280	0.386	0.308	0	6	1	1/2.56

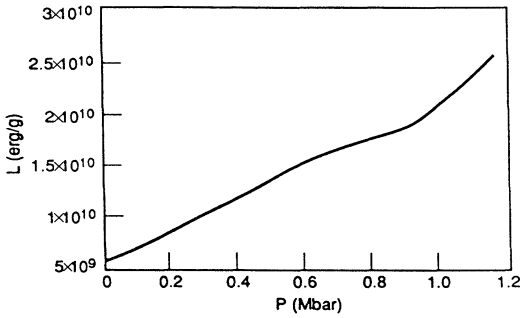

FIG. 2. The latent heat (L) of aluminum as a function of the pressure (P) on the melting (MC) of Fig. 1.

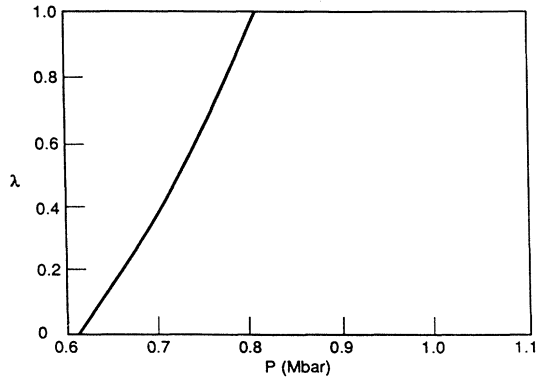

FIG. 3. The fraction (λ) of the solid to liquid phase transition after the shock-wave release in solid aluminum.

occurs at shock compressions of 790 kbar. This pressure is significantly below the Hugoniot pressure required for phase transition during the compression stage (~ 1.3 Mbar).

As suggested in Eq. (2) the above phase transition can take place for laser-induced shock waves about a nanosecond in duration. However, with the advent of very short laser pulses [15,16] (femtosecond pulses) it is possible to achieve high pressures during very short time duration, much shorter than the characteristic melting time scale. In this case the material will follow the solid adiabat beyond the melting curve as a "supercooled solid" and no melting will occur (for example, the adiabat 2-2″ of Fig. 1). If the material evolves in this way then the entropy on the Hugoniot curve can be calculated from the zero-pressure entropy of the solid.

In order to distinguish between the two thermodynamic routes, melting during the shock-wave release or solid supercooling the following experiments are suggested. The reflectivity R of the rear surface of the shocked target might be measured by optical backlighting [17]. R can be calculated, for example, from the Fresnel formula:

$$R=\frac{4\pi\sigma/\omega+1-2(2\pi\sigma/\omega)^{1/2}}{4\pi\sigma/\omega+1+2(2\pi\sigma/\omega)^{1/2}}\ , \tag{14}$$

where ω is the optical backlighting laser frequency and σ is the electrical conductivity given by

$$\sigma=\lambda\sigma_l+(1-\lambda)\sigma_s\ , \tag{15}$$

where σ_l and σ_s are liquid and solid conductivities accordingly. Taking into account that the ratio $\sigma_s/\sigma_l\sim 2$ in the neighborhood of the melting curve, a change in reflectivity of about 10% is obtained due to melting for the 0.25-μm wavelength laser. Moreover, multiwavelength measurements are necessary in order to isolate the melting phenomenon, as suggested by Reitze, Ahn, and Downer [18]. Such a reflectivity measurement requires very fast temporal resolution (~ 10 ps or less) and high accuracy since a decrease in reflectivity is expected also due to unloading of the material.

A second possible melting-detection experiment is the density measurements using extended x-ray-absorption fine structure (EXAFS) [19,20]. This technique determines the atomic spacing in a solid and liquid and therefore permits a direct evaluation of the densities ρ_s and ρ_l. The EXAFS method has been used widely to investigate the atomic arrangement of static materials and melting phases [21] and recently to the measurement of transient phenomena, such as ion-correlation effects in a dense shock-compressed plasma [19].

Another interesting experiment would be an accurate temporal measurement of the rear temperature during the relaxation of the shock wave [7]. As it can be seen from Fig. 1 the temperature pressure dependence and therefore the temperature time dependence is changing at point i if the system starts to evolve along the melting curve on the path $i\rightarrow 2'$. So the start of melting corresponds to a kink in the temporal temperature curve. Therefore the presence or absence of a kink on the experimental temporal temperature curve may confirm that the metal is melting.

In summary, the melting fraction in a shocked aluminium was calculated as a function of the Hugoniot pressure. Moreover, it is suggested that a "supercooling" phenomenon without melting might be possible for very short duration shock waves. Such pressure profiles can be created with very short high-irradiance laser pulses. Some experiments suggested here with different laser-pulse duration may clarify the time scale of solid to liquid phase transitions.

We are grateful to Dr. Y. Paiss for very useful and illuminating discussions.

[1] S. Eliezer, A. Ghatak, and H. Hora, *An Introduction to Equations of State: Theory and Applications* (Cambridge University Press, Cambridge, England, 1986).

[2] *High Pressure Equations of State: Theory and Applications,* Proceedings of the International School of Physics "Enrico Fermi," Course 113, edited by S. Eliezer and R. A. Ricci (North-Holland, Amsterdam, 1991).

[3] J. M. Besson, in *High Pressure Equations of State: Theory and Applications* (Ref. [2]).

[4] M. Ross, in *High Pressure Equations of State: Theory and*

Applications (Ref. [2]).
[5] R. M. McQueen, in *High Pressure Equations of State: Theory and Applications* (Ref. [2]).
[6] A. V. Bushman, V. E. Fortov, and I. V. Lomonosov, in *High Pressure Equations of State: Theory and Applications* (Ref. [2]).
[7] A. Ng, D. Parfeniuk, and L. DaSilva, Phys. Rev. Lett. **54**, 2604 (1985).
[8] R. Fabro *et al.,* Laser Part. Beams **8**, 73 (1990).
[9] H. Szichman and S. Eliezer, Laser Part. Beams **10**, 23 (1992).
[10] V. D. Urlin, Zh. Eksp. Teor. Fiz. **49**, 485 (1965) [Sov. Phys. JETP **22**, 341 (1966)].
[11] B. Arad *et al.,* Plasma Phys. Controlled Fusion **26**, 845 (1984).
[12] H. M. Driel and K. Dworshak, Phys. Rev. Lett. **69**, 3487 (1992).
[13] L. V. Altshuler *et al.,* Zh. Eksp. Teor. Fiz. **73**, 1866 (1977) [Sov. Phys. JETP **46**, 980 (1977)].
[14] S. B. Konner and V. D. Urlin, Dokl. Akad. Nauk SSSR **131**, 542 (1960) [Sov. Phys. Dokl. **5**, 317 (1960)].
[15] H. M. Milchberg *et al.,* Phys. Rev. Lett. **61**, 2364 (1988).
[16] A. Zigler *et al.,* Appl. Pys. Lett. **59**, 534 (1991).
[17] A. Ng *et al.,* Phys. Rev. Lett. **57**, 1595 (1986).
[18] D. H. Reitze, H. Ahn, and M. Downer, Phys. Rev. B **45**, 2677 (1992), and references therein.
[19] T. A. Hall *et al.,* Phys. Rev. Lett. **60**, 2034 (1988); B. A. Shiwai *et al.,* Laser Part. Beams **10**, 41 (1992).
[20] R. W. Eason *et al.,* Appl. Phys. Lett. **47**, 442 (1985).
[21] P. J. Mallozzi *et al.,* Phys. Rev. A **23**, 824 (1981).